




# Ocean state forecasting during VSCS Ockhi and a note on what we learned from its characteristics: A forecasting perspective

R HARIKUMAR<sup>1,\*</sup> , P SIRISHA<sup>1</sup>, ANURADHA MODI<sup>1,2</sup>, M S GIRISHKUMAR<sup>1</sup>, S VISHNU<sup>1,3</sup>, K SRINIVAS<sup>1</sup>, RAKHI KUMARI<sup>1</sup>, G YATIN<sup>1</sup>, P DINESH KUMAR<sup>1</sup>, T M BALAKRISHNAN NAIR<sup>1</sup> and M MOHAPATRA<sup>4</sup>

<sup>1</sup>Indian National Centre for Ocean Information Services, Ministry of Earth Sciences, Govt. of India, Hyderabad 500 090, India.

<sup>2</sup>Kerala University of Fisheries and Ocean Studies (KUFOS), Kochi 682 506, Kerala, India.

<sup>3</sup>Earth and Planetary Science Department, University of California, Berkeley, California, USA.

<sup>4</sup>India Meteorological Department, Mausam Bhawan, Lodhi Road, New Delhi 110 003, India.

\*Corresponding author. e-mail: harikumar@incois.gov.in harikumarraj@gmail.com

MS received 23 April 2021; revised 13 December 2021; accepted 14 December 2021

Tropical Cyclone Ockhi was an intense cyclone, with a peculiar and long track, in the Arabian Sea in 2017. It caused severe damage to coastal infrastructure and death of 282 people. Indian National Centre for Ocean Information Services (INCOIS) issued the Joint INCOIS-IMD (India Meteorological Department) bulletins on the Ocean State Forecasts (OSF) and alerts/warnings during Ockhi. Validation of the OSF from INCOIS using buoys reveals that the forecasts were in good agreement with the observations [average correlation 0.9, RMSE <0.8 m (for larger waves), and scatter index <25%]. Climatological analysis of Genesis Potential Index (GPI) suggests that the southeast Arabian Sea, where the TC-Ockhi was intensified, had all the favourable conditions for intensification during November/December. Moreover, it was found that four days before the genesis of Ockhi, the environmental vorticity and relative humidity were more favourable for the cyclogenesis compared to vertical wind shear and potential intensity. The intensification rate was rapid as experienced by earlier cyclones in this region. Also, the cyclone track closely matched the background tropospheric winds. The present study suggests that the forecasters should look into the background dynamic and thermodynamic conditions extensively in addition to multi-model guidance to better predict the genesis, intensity and track of the cyclones.

**Keywords.** Tropical Cyclone Ockhi; Ocean State Forecasting (OSF); rapid intensification; Genesis Potential Index (GPI); oceanic warnings and alerts.

## 1. Introduction

Tropical cyclones (TC) are the most frequently occurring natural hazards affecting the Indian Ocean and its rim countries. The disastrous consequences of the TCs are very high winds and

waves, floods associated with heavy rains and storm surges, inundation, erosion, along with loss of life, casualties, and damage to the properties causing huge socio-economic loss (Akhila and Anna Durai 2018). Hence, early warnings and alerts based on ocean state forecasting, along with

real-time monitoring have a significant role along the Indian coast and its island territories. TC warnings or alerts provide detailed information about the intensity of the cyclonic storm, position, direction of movement, future direction and intensity of the storm and landfall positions. Real-time monitoring and early warnings/alerts during the storm conditions are highly challenging tasks as the TCs can be varying in intensity and change path dynamically during its active life span. India Meteorological Department (IMD) issues the cyclone warning in terms of its intensity, track and storm surges, while the warning on the conditions in the sea such as associated high waves, swells and ocean currents are issued by Indian National Centre for Ocean Information Services (INCOIS), Ministry of Earth Sciences, Government of India. However, complete forecasts on cyclone intensity, track, landfall, ocean state such as waves, swell, surface currents, storm surges are issued and disseminated to the end-users in the form of INCOIS-IMD joint bulletins ([https://incois.gov.in/WEB\\_SITE\\_FILES/OSF\\_FILES/forecast/Bulletins](https://incois.gov.in/WEB_SITE_FILES/OSF_FILES/forecast/Bulletins)). INCOIS has been issuing warnings during all the cyclones since 2007 (Balakrishnan Nair *et al.* 2013). Most of these cyclonic storms were accompanied by huge waves and storm surges, devastating winds and high precipitation, resulting in the inundation of low-lying areas. The methodology and accuracy of the Ocean State Forecasts (OSF) generated at INCOIS is described in detail in Balakrishnan Nair *et al.* (2013, 2014), Harikumar *et al.* (2015), Hithin *et al.* (2015) and Sirisha *et al.* (2015, 2017).

Generally, the west coast of India has been witnessing fewer TCs than the east coast, typically for every four cyclones crossing the east coast, the west coast experiences one, as evidenced from a climatological analysis (Girishkumar and Ravichandran 2012). The TC-Ockhi (November 29–December 6, 2017) formed in the BoB and emerged in the AS, killing 174 fishermen from Kerala and 108 fishermen from Tamil Nadu, already ventured into the open ocean (Thara 2018). The economic loss caused by TC-Ockhi is estimated to be around US \$5.07 Billion. In general, the loss of lives and property during cyclones occurs near the landfall point and time. On contrary, in the case of TC-Ockhi, loss of lives and property was occurred out at the open ocean because the fisher folks ventured offshore even before the low pressure was formed, and moreover, there was no means to send the cyclone forecasts and information to the seafarers,

who were already out at the open ocean. TC-Ockhi is the first system in almost 40 years, which travelled about 2,400 km from the southern part of BoB to Gujarat (IMD 2017). The Very Severe Cyclonic Storm (VSCS) TC-Ockhi developed from a low-pressure area over southwest BoB and adjoining areas of south Sri Lanka and equatorial Indian Ocean in the forenoon of 28th November (figure 1). It became a well-marked low-pressure area in the early morning of 29th over the same region. It further concentrated into a Depression (D) over southwest BoB off southeast Sri Lanka coast in the forenoon of 29th November, moving westward, it crossed Sri Lanka coast after some time. Continuing its westward movement, it emerged into Comorin area in the evening of 29th November and intensified into a Deep Depression (DD) in the early hours of 30th November. It further moved northwestwards and intensified into a Cyclonic Storm (CS) in the forenoon of 30th November over the Comorin area (IMD 2017). While moving west–northwestwards, it further intensified into a Severe Cyclonic Storm (SCS) over Lakshadweep area in the early morning of 1st December and into a VSCS over southeast AS to the west of Lakshadweep in the afternoon of 1st December. It then moved northwestwards and reached its peak intensity of 150–160 kmph gusting to 180 kmph in the afternoon of 2nd December with lowest central pressure of 976 hPa. It moved

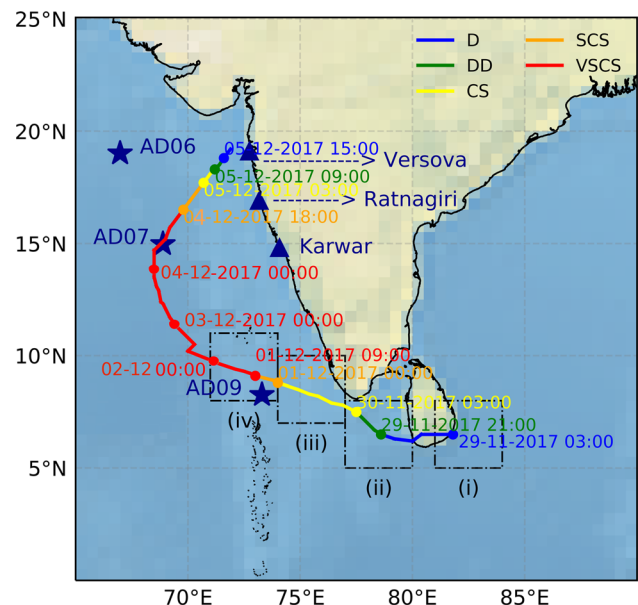


Figure 1. Track of TC-Ockhi (November 29–December 6, 2017) as reported by IMD. Locations of the open ocean moored buoys and coastal directional wave rider buoys are marked with star and triangle symbols, respectively.

north–northwestwards for some time and then north–northeastwards and maintained its intensity till early morning of 3rd December. It then continued to move north–northeastwards and weakened gradually. It crossed the south coast of Gujarat between Surat and Dahanu as a well-marked low around early morning of 6th December.

TC-Ockhi was projected as a rare TC with rapid intensification in the genesis stage over northern Indian Ocean. It intensified from DD into a CS over Comorin area within 6 hrs. From the historical data of the TC records, one can notice that, in general, cyclones that formed in the southeast AS used to travel westwards and make a landfall near Oman or Persian Gulf (such as cyclones Gonu, Yemyin and Phet). These cyclones moved towards offshore areas of AS and intensified further into VSCS category. But the case of TC-Ockhi is entirely different; once it entered into the AS, it intensified very quickly and attained a VSCS status.

In the present study, firstly, we have analyzed and assessed the ocean state forecasts generated at INCOIS using a numerical spectral wave model using the available moored buoys and Directional Wave Rider Buoys [DWRB; under the WAVE Monitoring Along Nearshore (WAMAN) buoy network programme of INCOIS] network (figure 1). Accurate ocean state forecasting using ocean models, especially during extreme weather conditions like cyclones, is dependent on accurate forcing fields, namely, atmospheric forecasts. If this aspect is not taken due care, there is a risk of underestimation of the wind and thereby wave fields, especially in extreme weather conditions like cyclones, where winds play a very important role. It is a common practice that weather and oceanic forecasting is improved by improving the model skills. In a similar fashion, it is also equally important to understand deeply about the dependence of the TC behaviour (in terms of genesis, intensity and track) and its strong correlation to the prevailed background atmospheric and oceanic conditions, to better predict the intensity and track of TCs. Keeping this important aspect in mind, the second objective of the present study is to unravel the characteristics of TC-Ockhi, in terms of its genesis, intensity and track compared to other cyclones in the past, in a forecasting perspective. This understanding will lead to a better refinement of the predictability of the genesis, intensity and track of the cyclones and all the associated

parameters like waves, storm surges and oceanic currents. In the present manuscript, quantitative assessment of the ocean state forecasts is done. How the background conditions were conducive for the genesis, intensification and track of the cyclone is also depicted. Bringing out these two concepts in the same manuscript would be of paramount importance and consequential applicability in refining the marine meteorological and ocean state forecasting.

### 1.1 Ocean state forecasting from INCOIS

INCOIS provides quantitative OSFs and advisory services to all the sea-faring communities like the fishermen, Indian Navy, Indian Coast Guard, merchant and passenger vessels, offshore oil and gas exploration agencies, research organisations and also to the coastal communities, local government authorities and disaster management authorities. Under the OSF services, INCOIS provides forecasts of wave heights, direction and period (of both wind sea and swell waves), sea surface currents, sea surface temperature, mixed layer depth (the well-mixed upper layer of the sea), depth of the 20°C isotherm (a measure of the depth of the thermocline), astronomical tides as well as wind speed and direction. During cyclones and other extreme weather conditions, based on the forecast information, alerts/warnings are issued to the general public as well as the Administrators/Disaster Management Authorities of the coastal stretch under risk, so that the population under threat is relocated to safer places or other safeguards are in place. High wave bulletins with alerts or warnings are helpful to the users, especially during extreme weather conditions, for taking precautions. From February 2014 onwards, the Joint INCOIS-IMD bulletins containing information on the probable locations along the coast where wave heights and current speeds are likely to be high because of the effect of depression or cyclone are being issued. Crucial quantitative information and advisories on high waves, tidal phases, currents along with fishermen warnings and advisories are presented in these bulletins. These also contain crucial information on meteorological parameters from IMD thereby providing complete information to the user communities, and hence such bulletins act as an integrated, unified and one-stop forecast, information and advisory package without any ambiguity.

INCOIS issued the Joint INCOIS-IMD bulletins on the OSFs and alerts/warnings for all the locations concerned and to all the users through multi-dissemination modes also during the life cycle of TC-Ockhi, right from its genesis to dissipation. INCOIS provides these services in local languages through different modes like INCOIS website, e-mail, mobile phones (through SMSs and Apps), TV, Radio, Electronic Display Boards and social media to all the stakeholders. All the Information and Communication Technology (ICT) tools have been exploited to the maximum for providing in-time quality forecasts to the wide user-communities. Further, there is strong collaboration with various NGOs (such as Reliance Foundation, MS Swami Nathan Research Foundation, IFFCO Kisan Sanchar Limited), coastal research centres as well as universities, for further awareness, training and dissemination to the end-users; and with local government authorities, State Disaster Management Authorities and National Disaster Management Authority for further decision making and actions.

## 2. Data and method

Wave forecasts were evaluated using open ocean moored buoys (namely AD06, AD07, AD09 are used in the present study) and coastal DWRBs (figure 1). It is evident that AD07 was located exactly on the cyclone track and AD09 was on the left side of the cyclone track. The generation of wave forecasts and related data is explained in detail in the next subsection. Genesis Potential Index (GPI), an empirical index for TCs (Emanuel and Nolan 2004; Camargo *et al.* 2007), is a function of most important environmental conditions such as low-level vorticity ( $\text{sec}^{-1}$ ), middle-level relative humidity (%), wind shear ( $\text{sec}^{-1}$ ) and potential intensity (m/sec). The GPI threshold used for delineating the chance for a cyclonic system to form or not is 0.05 for the global tropical regions (Zhang *et al.* 2019). GPI analysis was carried out using NCEP (1979–2017; National Centre for Environmental Prediction; Kalnay *et al.* 1996) and ERA (ECMWF Re-Analysis)-Interim (1979–2018; Dee *et al.* 2011) reanalysis datasets. The tropospheric wind data also have been taken from NCEP (Kalnay *et al.* 1996). Maximum sustained wind speed data during the TC-Ockhi period have been taken from IMD (2017). Data on the cyclones from 1980 were taken from the IMD E-Atlas (<http://www.rmccennaieatlas.tn.nic.in>).

### 2.1 Wave forecasts – numerical wave model and its forcing parameters

During the TC-Ockhi, INCOIS issued the wave forecasts and warnings, which were generated using third-generation Spectral wind-Wave model MIKE21 SW (SW). This model is based on unstructured meshes, and hence it takes into account all the important phenomena like wave growth by influence of wind, nonlinear wave–wave interaction, dissipation of wave energy due to white-capping, bottom friction and depth-induced wave breaking, refraction and shoaling due to depth variations and wave–current interaction. SW was found to perform well during the cyclone period (Balakrishnan Nair *et al.* 2013). The model domain, mesh resolution and bathymetry are shown in figure 2. A fine resolution mesh of  $0.045^\circ$  was used along the west coast, whereas a coarse resolution mesh of  $0.25^\circ$  was used in the offshore areas of the AS. A coarse resolution mesh of  $1^\circ$  was used in the remaining areas of the Indian Ocean. The pre-processing steps of the model simulation are also explained in detail in Balakrishnan Nair *et al.* (2013).

In general, third-generation wave models underestimate the wave heights, especially during rapidly varying cyclonic conditions. To address this underestimation in wave height, we have been using a calibrated setup of the SW which yields good results during cyclones (Balakrishnan Nair *et al.* 2013). This calibration works fine for the coastal region and offshore region, but not for the entire basin. Moreover, the white capping tuned in the setup still has some extent of dissipation which results in some underestimation in wave height. The SW model was forced with ECMWF (European Centre for Medium-Range Weather Forecasts) forecast winds from 27th November–1st December, 2017, and the outputs and initial conditions were saved from this simulation. The magnitude of the wave height in third-generation wave models is strongly dependent on the magnitude of the forcing wind speed. Therefore, this underestimation in the input wind will cause underestimation in the forecasted wave fields, rendering the forecast inaccurate, hence not useful in the operational context. The error correction of the wind input is a high priority in operational context, especially during cyclones, to get more accurate wave simulations. For this purpose, we have done the bias correction to the input winds following Harikumar *et al.* (2016). The model was



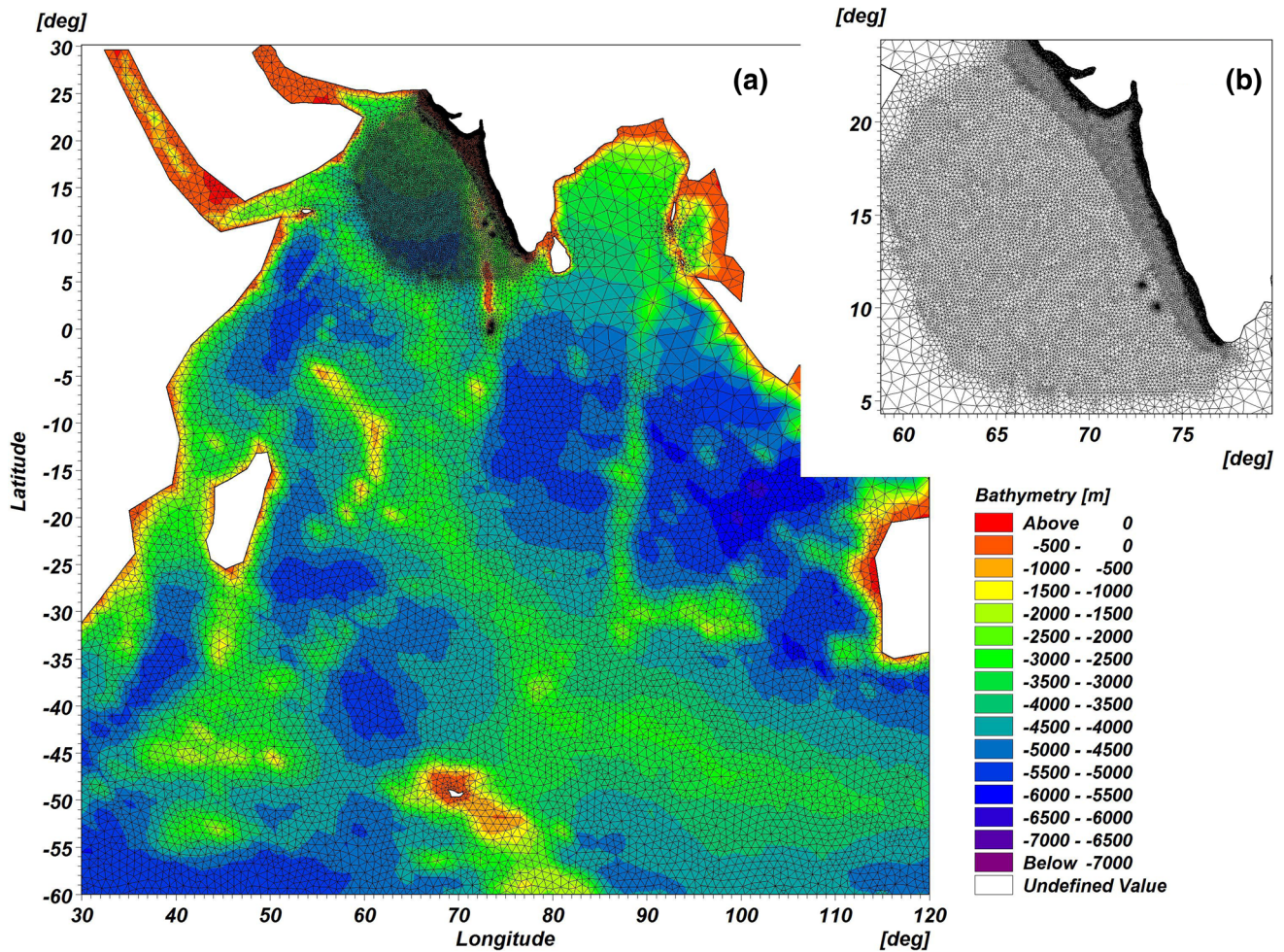


Figure 2. (a) SW model domain, bathymetry and mesh used in the forecast system and present study and (b) fine resolution mesh used in the AS.

run by forcing it with the bias-corrected ECMWF forecast winds (1st–7th December, 2017) taking initial condition from the previous day’s run, and the forecasts and warnings were issued.

### 3. Results and discussion

#### 3.1 Evaluation of ocean state forecasts

Characteristics of wave during the lifespan of the TC-Ockhi is explained below. Figure 3 shows spatial plots of forecasted significant wave height ( $H_s$ ) during TC-Ockhi period, at some crucial timings. Figure 3(a) shows the TC-Ockhi generated wave fields near the coastal areas of Kanyakumari, southwest Tamil Nadu and Sri Lanka on 29th November 2100 UTC. From the overlaid cyclone track, it is evident that the system as a deep depression has entered southwest AS on 30th November 0300 UTC (figure 3b), which caused a

rapid change in the wave field, within 6 hrs. It is evident from figure 3(a and b) that the track of the cyclone has changed and it has entered into the southwest AS. Further, figure 3(c and d) shows the wave fields associated with the rapid intensification of cyclone from CS to VSCS (within a span of 3 hrs) on 30th November in the southeast AS. The coastal areas which are located on the right side of the cyclone track are affected more by the cyclone waves in the north Indian Ocean (Sirisha *et al.* 2015). Major destruction was noticed in the case of Lakshadweep Archipelago, which is located on the right side of the cyclone track (figure 1). Once the cyclone intensified to VSCS in the southeast AS, the speed of the cyclone reduced near the Lakshadweep islands and devastated this region from 1st to 3rd December (figure 1). The low-lying areas of the islands were reported to be highly inundated. However, the devastation caused by TC-Ockhi to these islands is beyond the scope of the present study. The alerts, warnings and general forecasts

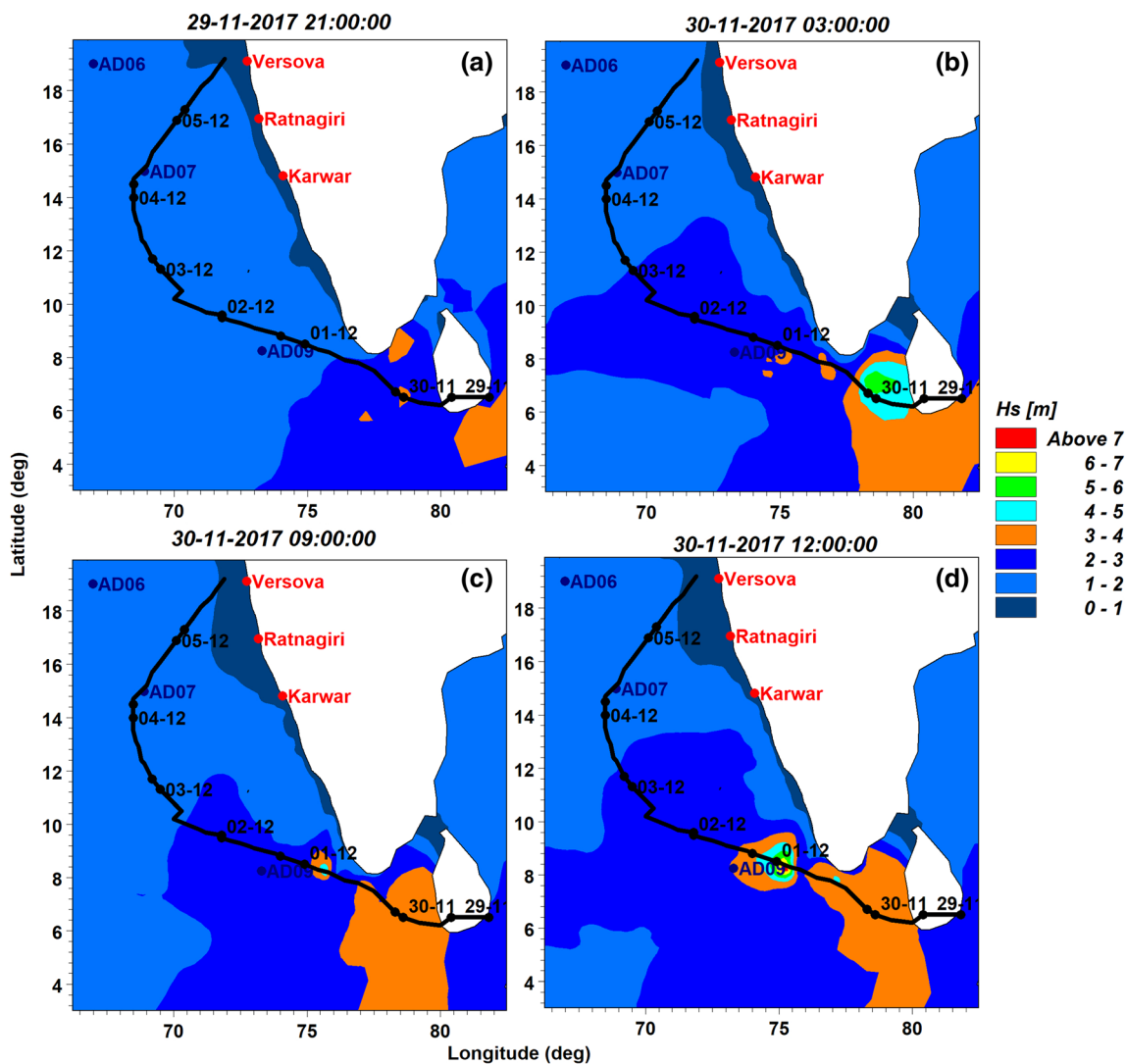


Figure 3. Typical plots of cyclone generated wave fields in the southeast AS (a) on 29th November 2100 UTC, (b) on 30th November 0300 UTC, (c) on 30th November 0900 UTC, and (d) on 30th November 1200 UTC. Track is overlaid and labelled with dates indicating the position of the system at 00:00 IST on each day.  $H_s$  [m] represents the significant wave height in metre.

have been issued 48 hrs prior to the cyclone occurrence, i.e., 28th November onwards to the coastal areas of southern Tamil Nadu, Kerala, Karnataka and Lakshadweep islands.

Evaluation of the wave forecasts was carried out with observations from three open ocean moored buoys (AD06, AD07, AD09; figure 1) and four coastal DWRBs (off Karwar, Ratnagiri and Versova). The forecasted wave parameters which were compared with observation are  $H_s$ , swell wave height ( $H_{ss}/H_{m0a}$ ), wind sea wave height ( $H_{sw}/H_{m0b}$ ), maximum wave height ( $H_{max}$ ), mean wave period ( $T_{m02}$ ), mean wave direction ( $M_{dir}$ ), wind speed (WS), and wind direction (WD). The location of AD06 is comparatively far from the cyclone track and AD07 data is discontinuous from 4th December onwards. The AD09 buoy has

continuous data and is closer to the cyclone track compared to the AD06 buoy. Hence we have selected AD09 buoy for displaying time series comparison, as shown in figure 4. Generally, the wave heights in the AS are predominantly low (1.5–2 m) during the northeast monsoon season (October–December) and January to March because of weak winds during this period. From figure 4(a), we can see the presence of low wave heights (<2 m) from 27th to 29th November in the observation data. Observed wave heights increased from 30th November onwards, whereas forecast has shown high wave heights from 1st December onwards. Thus, a slight shift in predicting high waves was noticed during the initial stage of the cyclone. This is because the forecast was generated using bias-corrected winds (following Harikumar

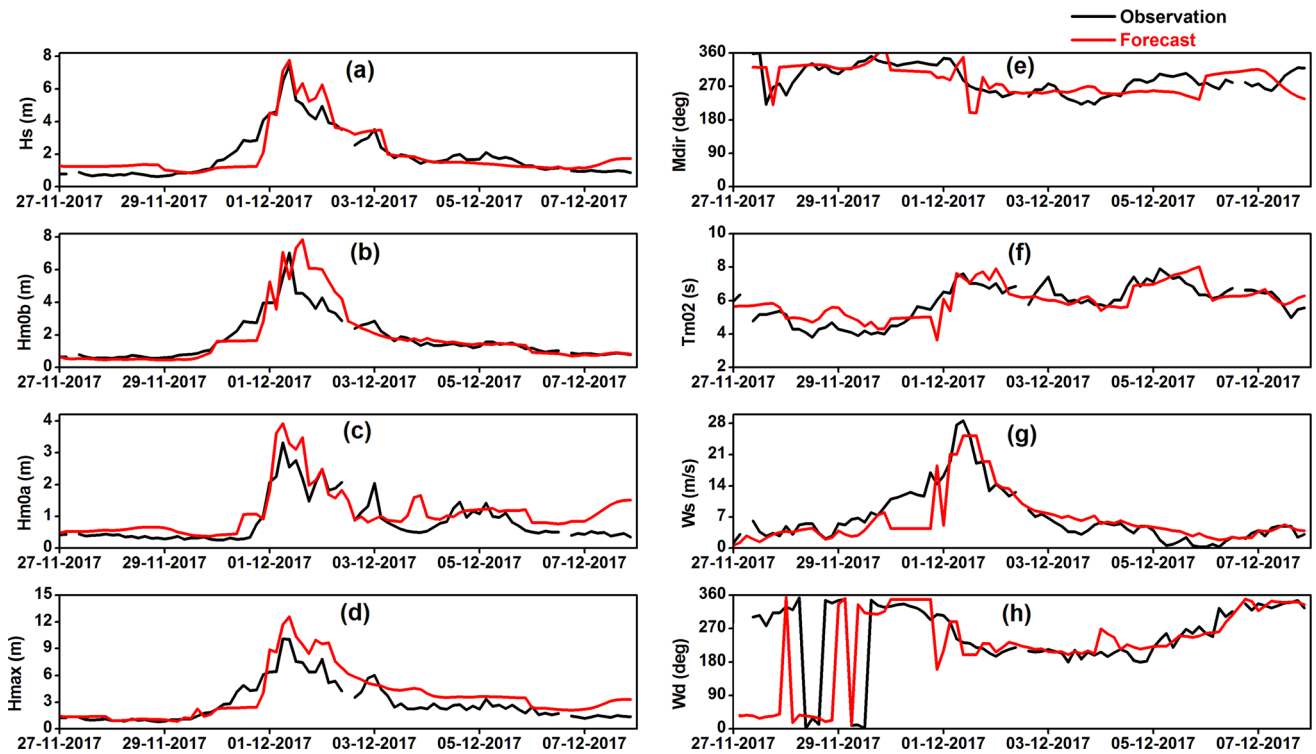


Figure 4. Time-series comparison of the forecasted wave parameters  $H_s$ ,  $H_{sw}/H_{m0b}$ ,  $H_{ss}/H_{m0a}$ ,  $H_{max}$ ,  $M_{dir}$ ,  $T_{m02}$  and wind speed and direction with buoy AD09 observations during the TC-Ockhi (27th November–7th December, 2017).

*et al.* 2016) only from 1st December onwards, after realizing that there is presence of a systematic underestimation in the ECMWF winds evidenced from the evaluation of simulations using real-time observations. The details and methodology of wind bias correction by taking TC-Hudhud as an example are explained in Harikumar *et al.* (2016). In this case of TC-Ockhi, the wind range in m/s (the multiplication factor applied to correct the bias) are 0–5 (no bias), 5–10 (1.02), 10–15 (1.15), 15–20 (1.2), 20–25 (1.25), 25–30 (1.3), 30–35 (1.35), 35–40 (1.45), >40 (1.5). On 1st December 0900 UTC, observed and forecasted  $H_s$  were 7.5 m and 7.8 m, respectively at AD09 location. There is a very good correlation with correlation coefficient of 0.9 between the observed and forecasted  $H_s$ . The cyclone track is very close to AD09 on 1st and 2nd December (figure 1), hence high wave heights are clearly noticed in the observation. The high waves forecasted are maintained at this location from 1st to 2nd December, then showed decreasing trend as that of observation (figure 4a). After 3rd December, both observed and forecast wave heights were <2 m, indicating calm wave regime at this location. Model has shown good response in reproducing the high and lower wave heights at AD09 during the TC-Ockhi period. The period 1st to 2nd December, showed highest values of  $H_{sw}$  ( $H_{m0b}$ )

6–7 m,  $H_{ss}$  ( $H_{m0a}$ ) of 3–4 m,  $H_{max}$  of 10–12 m, in the observation and forecast (figure 4b, c and d). Model was able to simulate the multiple peaks of the swell (figure 4c) and slightly overestimated the wind seas (figure 4b) at the peak. The  $H_{max}$  from the model has slightly overestimated from 1st to 7th December continuously. The propagation of waves from northwest to north is seen at this location during 27th–30th November (figure 4e). But once the cyclone approached this location, i.e., on 1st–2nd December, the wave propagation observed was mostly from southwest and west directions. The forecast has shown good agreement in simulating the change in wave propagation direction during the cyclone period. The time series comparison of peak wave period (figure 4f) shows good agreement of forecast with observation during the entire period (4–8 s).

The observed and bias-corrected forecast wind speed has shown the highest value (of 28.7 and 25.7 m/s, respectively) on 1st December 0900 UTC, at AD09 location (figure 4g). Both observed and forecasted winds were in the range of 15–28 m/s on 1st–2nd December and decreased afterwards. The wind directions are north and northwest from 27th to 30th November and suddenly changed to south and southwest on 1st–2nd December, as can be expected in a time series during the passage of



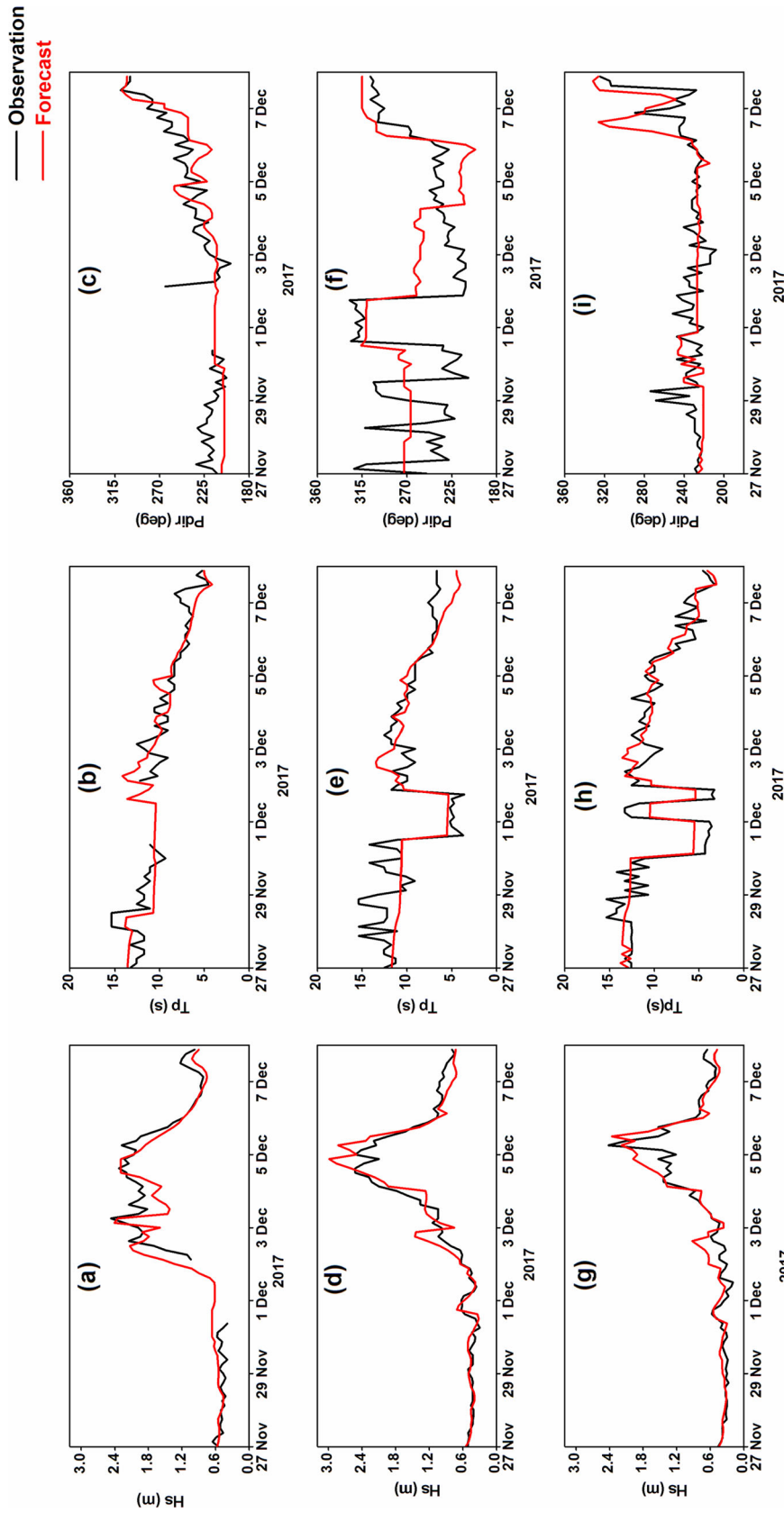


Figure 5. Time-series comparison of the forecasted wave parameters Hs, Tp and Pdir at Karwar (a–c), Ratnagiri (d–f) and Versova (g–i).



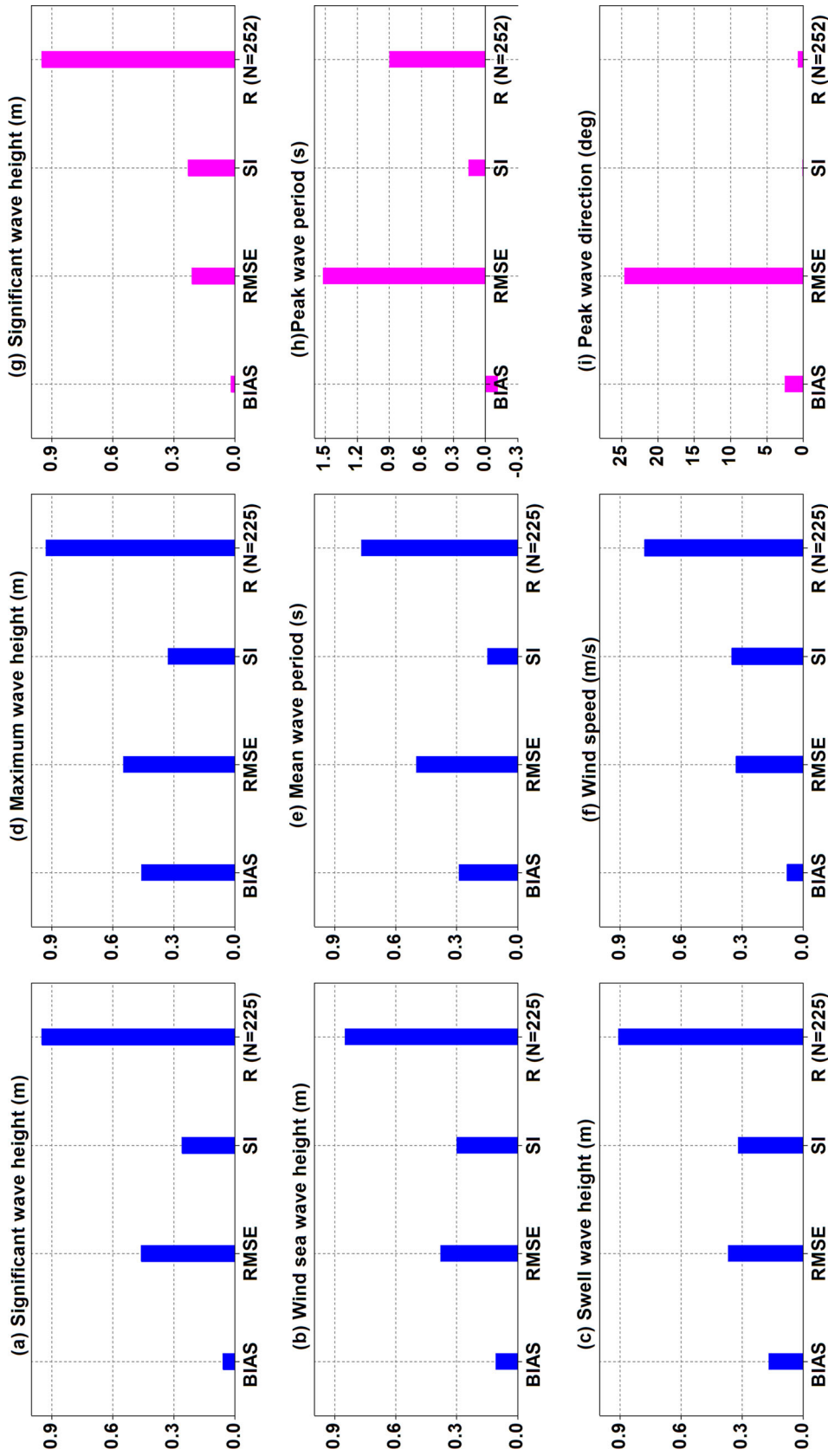


Figure 6. Bulk error statistics computed for the open ocean regime of AS (a-f) and west coast of India (g-i) during TC-Ockhi.

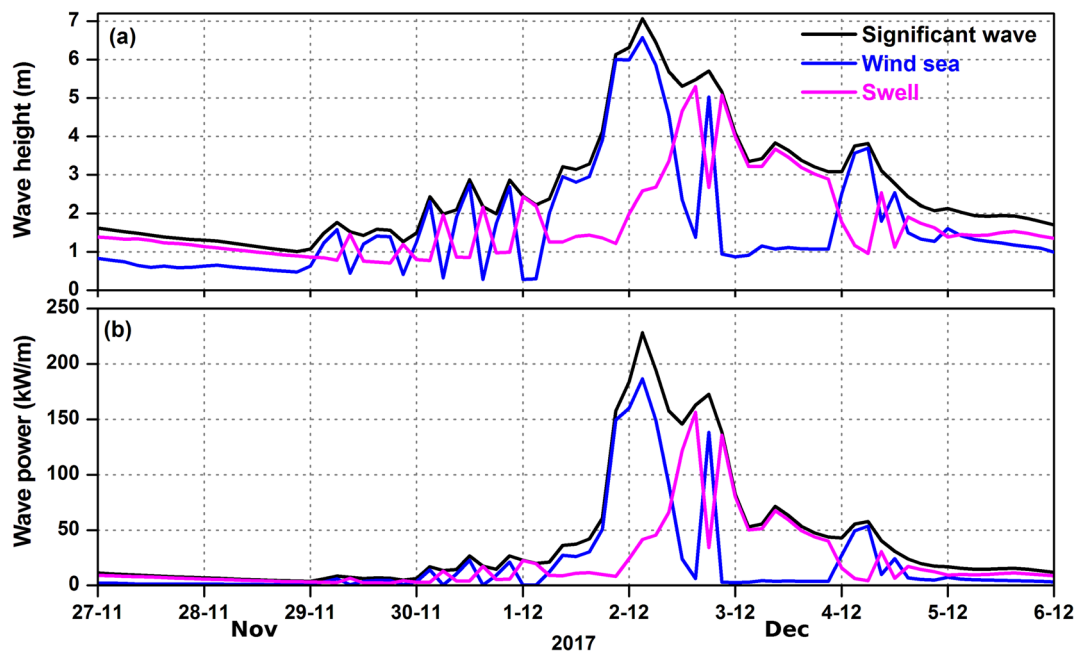


Figure 7. Time series plots of forecasted wave height and wave power off Agatti Island during TC-Ockhi.

any cyclone through the point of buoy observation location (figure 4h). The magnitude of forecast winds and directions were in good agreement with the observations (figure 4g, h). However, it is worth mentioning here that, the wind speed was underestimated on 30 November. Henceforth, the winds were in good agreement as the correction was initiated December 1 onwards, after realizing a remarkable underestimation on the previous day. It is also consistent with the comparison of the wave forecast time series with observation as seen in figure 4(a).

Figure 5 shows the time series plots of the wave forecast comparison  $H_s$ ,  $T_p$  (peak wave period) and  $P_{dir}$  (peak wave direction) with observation near the coastal areas of Karwar (figure 5a–c), Ratnagiri (figure 5d–f) and Versova (figure 5g–i).  $H_s$  from observation has shown peak value of  $\sim 2.5$  m at Karwar on 3rd–5th December and Ratnagiri and Versova (figure 5g–i) on 4th–5th December. Though these coastal areas are located on the right-hand side of the cyclone track, very high waves (with wave heights  $>3$  m) were not present during the cyclone period. It is observed that the coastal areas of Karwar, Ratnagiri and Versova were not severely affected by the cyclone. TC-Ockhi has weakened after 3rd December, that is, once it crossed the Lakshadweep islands. Though the cyclone persisted in the AS, the strength of the cyclone had decreased from VSCS to CS, making the coastal areas of Karnataka and Maharashtra

less vulnerable to the cyclone. By the time the TC-Ockhi reached Gujarat, it had weakened completely and transformed to a depression stage. But the case of Kerala was different, as the cyclone had intensified from CS to VSCS on 1st December off Kerala and Lakshadweep, which caused loss of life and property of fisherman at sea during the period 30th November–3rd December. Except Kerala, southern Tamil Nadu and the Lakshadweep Archipelago, remaining coastal areas of the west coast were not severely affected by TC-Ockhi.

Forecasted  $H_s$  was able to reproduce all the peaks at the coastal areas during this cyclone (figure 5a, d and g).  $T_p$  from observation shows 7–12 s at Karwar (on 3rd–5th December, when waves are high), which is an indication of the coexistence of cyclone generated swells and wind waves, while that is only 7–8 s at Versova and Ratnagiri on 5th December (the day showed high waves), i.e., presence of only wind seas. The forecasted  $T_p$  agreed well with observation at these coastal areas (figure 5). Observed  $P_{dir}$  shows that the waves propagated along the southwest direction to the coastal areas during the cyclone period. The forecast  $P_{dir}$  at all coastal areas has shown good agreement with observation (figure 5).

Figure 6 shows bulk error statistics computed from the comparison of ocean state forecasts with all the available observations in the open ocean regime of AS (figure 6a–f) and west coastal regime of India (figure 6g–i). The wave model forced with

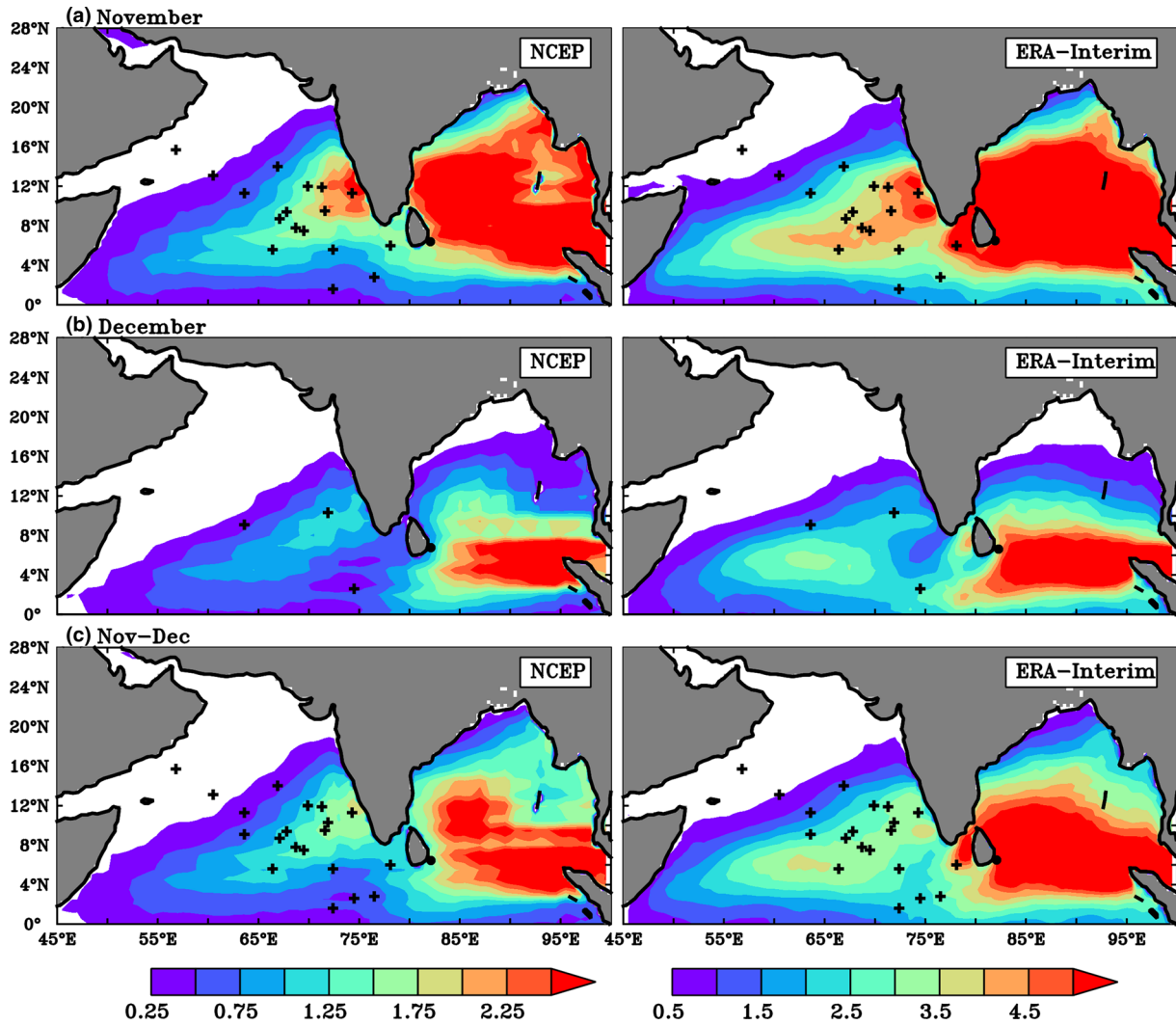


Figure 8. Spatio-temporal evolution of GPI climatology during post-monsoon season [derived from NCEP (left panel) and ERA-Interim (right panel)]. AS TC genesis locations are marked + (plus) symbol. Genesis location of the TC-Ockhi is marked as a black dot (off southeast of Sri Lanka).

bias-corrected ECMWF winds resulted in very less bias ( $<0.2$  m in wave heights) in the wave parameters ( $H_s$ ,  $H_{sw}$ ,  $H_{ss}$  and  $T_{m02}$ ), except for the  $H_{max}$  in the AS (figure 6a–f). RMSE values varied from 0.33 to 0.36 m in case of  $H_s$ ,  $H_{sw}$  and  $H_{ss}$  and a high RMSE of 0.55 m is noticed for  $H_{max}$ . Bias-corrected winds showed good agreement with the observation with a bias of only 0.08 m/s and RMSE of 0.33 m/s in the AS (figure 6f). The scatter index for all the wave parameters was in the range of 15–30% with  $r$  values varying from 0.78 to 0.95 suggesting a good agreement of the forecast in the AS (figure 6a–f). The reason for high bias and RMSE for only  $H_{max}$  is due to a slight overestimation of the model at AD09 location during this cyclone period.

The error statistics near the coastal areas are given in figure 6(g–i). Forecasted waves have bias

in the range  $\sim 0.02$  m for  $H_s$ , 0.14 s for  $T_p$ ,  $0.33^\circ$  for  $P_{dir}$  and RMSE values were in the range 0.2 m for  $H_s$ , 1.5 s for  $T_p$  and  $24^\circ$  for  $P_{dir}$ . The scatter index varied from 16 to 22% with high correlation of 0.76–0.95 suggests a good agreement of the forecast in the coastal areas also during this cyclone period.

### 3.2 Variation of wave power off Agatti Island

Lakshadweep Islands faced the brunt of the cyclone, being in the vicinity of the cyclone path. The small and scattered low-lying islands bore the impact in terms of high winds, huge waves, swell surges and consequential inundation. Hence, we have made an attempt to study the wave power near the Lakshadweep islands during the cyclone period. Figure 7 shows time series plots of the

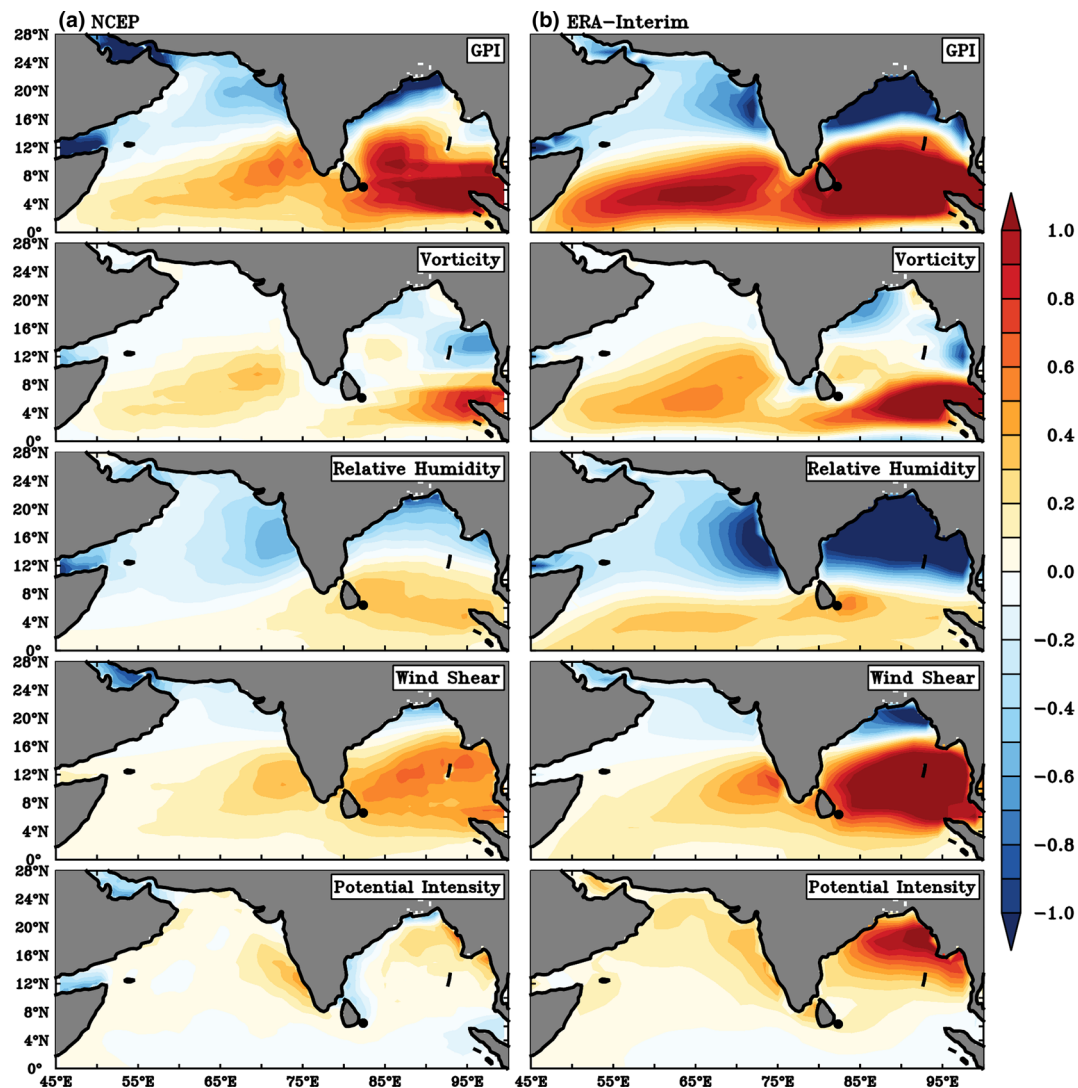


Figure 9. Change in GPI and respective terms (vorticity, relative humidity, wind shear and potential intensity) during November–December compared to the annual mean, from NCEP (derived using 1979–2017 data, left panel) and ERA-Interim (derived using 1979–2018 data). Genesis location of the TC-Ockhi is marked as a black dot (off southeast of Sri Lanka).

significant wave height, wind sea height, swell height and wave power off Agatti Island. It is evident from the figure that before the TC-Ockhi as a VSCS approached this location, i.e., from 27th to 30th November, the significant wave height was contributed from wind sea height and swell height (figure 7a). As the cyclone approaches the islands, i.e., from 1st to 2nd December, significant wave height was largely contributed from wind sea height. As soon as the cyclone has passed, that is, 4th–7th December, again the significant wave height was normally contributed by wind sea height and swell height. The wave power also follows the same trend (figure 7b) as that of significant wave height, that is, before and after the arrival of the cyclone, the total wave power near the Agatti Islands is contributed from both wind

sea and swell. But during the cyclone period (1st–2nd December), the major contribution was from wind sea only. The wave power is computed using the wave height and hence the trends are similar, as expected. The contribution from the wind sea component was dominant in the total wave power during the cyclone period. Further, the model has forecasted the highest significant wave height of 7 m and wave power of 230 kW/m near the Agatti Island during the cyclone period.

### 3.3 Characteristics of TC-Ockhi in terms of its genesis, intensity, track and differences/similarities with past cyclones

Understanding deeply about the characteristics of TC and the prevailing background atmospheric



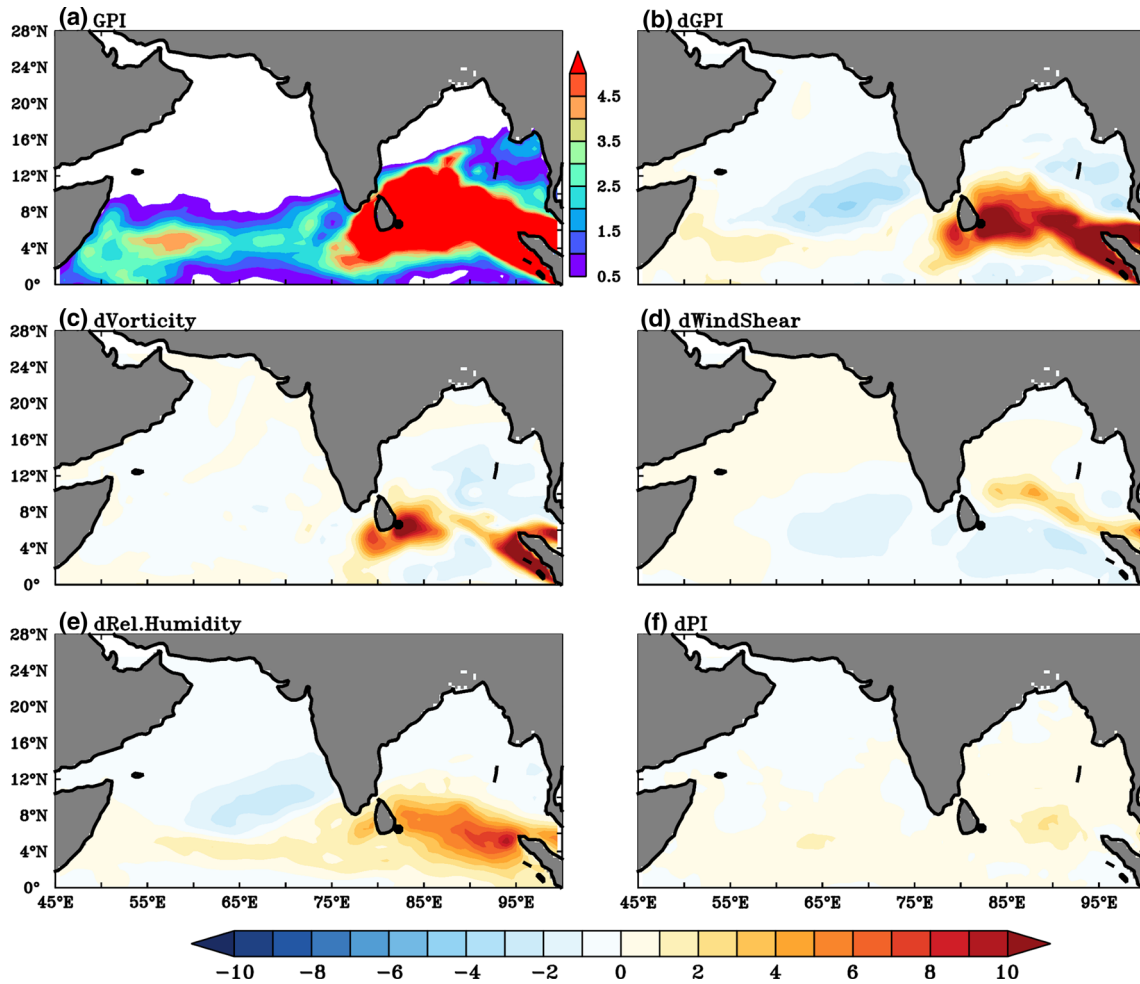


Figure 10. GPI (a), anomaly in the GPI (dGPI) and respective terms (vorticity, wind shear, relative humidity and potential intensity) during pre-TC-Ockhi period (24–28 November 2017) (b–f). The colour scale below is common for the five different parameters (b–f). Genesis location of the TC-Ockhi is marked as a black dot (off southeast of Sri Lanka).

and oceanic conditions are very important to better refine the predictability of the genesis, intensity and track of the TCs and all the associated parameters such as waves, storm surges and oceanic currents. Keeping this aspect in mind, in this section, we investigate the background atmospheric and oceanic conditions that lead to the formation, intensification and movement of TC-Ockhi and how did those background conditions differ with respect to the seasonal climatology. Subsequently, we studied on the genesis of TC-Ockhi, its track and intensification rate, to address whether TC-Ockhi’s life cycle had any significant difference with respect to overall TC activity in the AS.

Estimates of oceanic and atmospheric variables have been carried out to understand the prevailing background conditions of TC-Ockhi using GPI. GPI is a function of most important environmental conditions such as low-level vorticity, middle-level

relative humidity, wind shear and potential intensity, which lead to the TC genesis and intensification (Emanuel and Nolan 2004). One of the advantages of the GPI is that it synthesizes the important environmental parameters into a single number. Moreover, it facilitates us to evaluate the relative contributions of these important environmental factors on TC activity. In the present study, the GPI analysis was carried out using NCEP (1979–2017; Kalnay *et al.* 1996) and ERA-Interim (1979–2018; Dee *et al.* 2011) reanalysis datasets.

Spatio-temporal evolution of GPI climatology during the post-monsoon season in the north IO is presented in figure 8. During November and December months, GPI is very high in the southeastern AS, south of Indian peninsula and east of Sri Lanka. Moreover, it is noticed that there is a strong spatial correspondence with high GPI and TC genesis location (shown overlaid in figure 8) during November–December in the AS. GPI in the

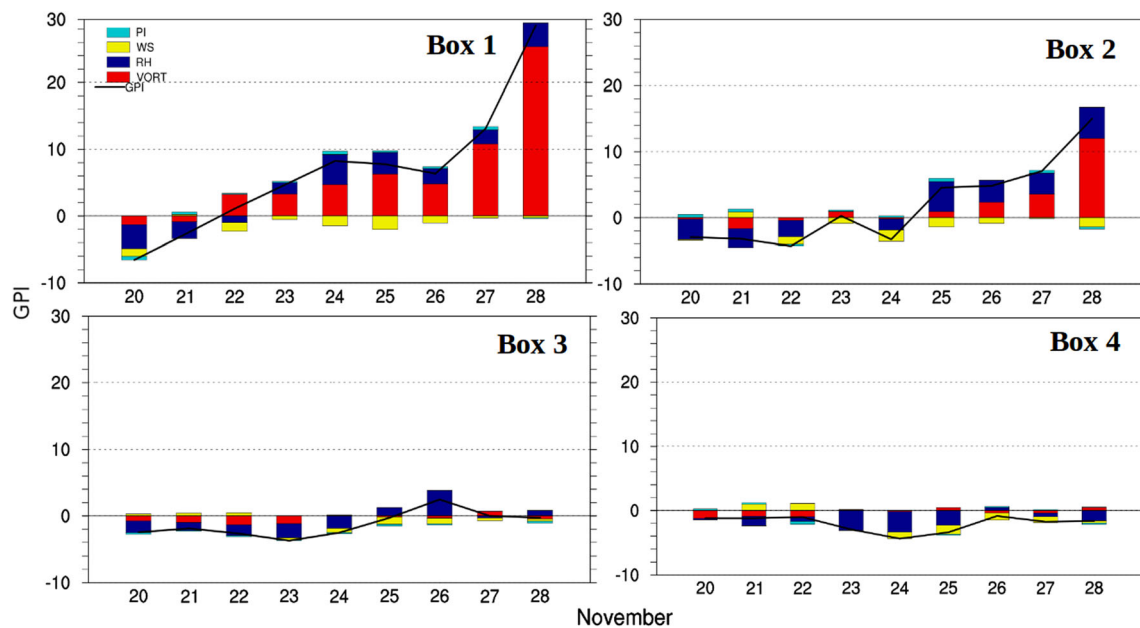


Figure 11. Temporal evolution of GPI anomaly during pre-TC-Ockhi period (20–28 November) in different boxes defined in figure 1. In the legend, PI, WS, RH, and VORT indicate potential intensity, wind shear, relative humidity, vorticity, respectively (ERA Interim data is used).

BoB is almost two times higher than that at AS during this season, which indicates, why BoB has more number of TC than AS (4:1) during post-monsoon season (Girishkumar and Ravichandran 2012). This is mentioned here because the low-pressure system of this cyclone was formed in BoB, the region east of Sri Lanka. In order to understand the relative contribution of various factors that lead to the peak TC activity in the AS, GPI anomaly based on seasonal mean is calculated following the methodology brought out by Li *et al.* (2013) and Girishkumar *et al.* (2015) (methodology is given in the Appendix). Our analysis revealed that the enhanced low-level cyclonic vorticity and suppressed vertical wind shear with respect to the annual mean lead to an enhanced GPI during November–December (figure 8c). It is worth mentioning here that, the above-derived parameters from both NCEP and ERA-interim datasets showed similar patterns. This indicates that, climatologically, these regions have large potential for the genesis and intensification of TC, mainly due to an enhanced low-level cyclonic vorticity and the reduction in vertical wind shear. This is consistent with the earlier studies in the AS (Evan and Camargo 2011). It is worth mentioning here that TC-Ockhi occurred during late November, the period of peak TC activity in the southeast AS on a seasonal time scale. Hence, it can be said that the genesis of TC-Ockhi in the southwest Bay of Bengal is not an unusual event.

The next question is what was the GPI condition in the Arabian Sea during TC-Ockhi period, and what are the factors that lead to the modulation of GPI with respect to the climatology during the similar period (figures 9 and 10). The GPI is relatively high during the TC-Ockhi period in the southeastern Arabian Sea, which is consistent with the GPI climatology (derived using 1979–2017 data) during the similar period. It is to be noted that the GPI anomaly (calculated from the daily mean) during pre-TC-Ockhi period (24–28 November 2017) shows significant anomalous high values only south of 8°N (figure 10).

TC-Ockhi, during its life span, transformed from one category to another along the track and became a VSCS by 1 December. A low-pressure system that formed east of Sri Lanka could succeed in crossing its mainland and entered into the southeastern AS as a depression. Further, its effect was felt drastically in the form of huge devastation to the southern and southwest parts of the Indian mainland during its course at that part during the first four days. The closest approach was 50 km offshore to the tip of the Indian peninsula. Moreover, on 27 November, there was no clear clue in the forecast about the ensuing intensification (IMD 2017). But, by 28 November, it was forecasted that there will be a fast and progressive intensification of the system during the ensuing days. Considering all these factors into account, we have classified the region at this part of the track into four spatial

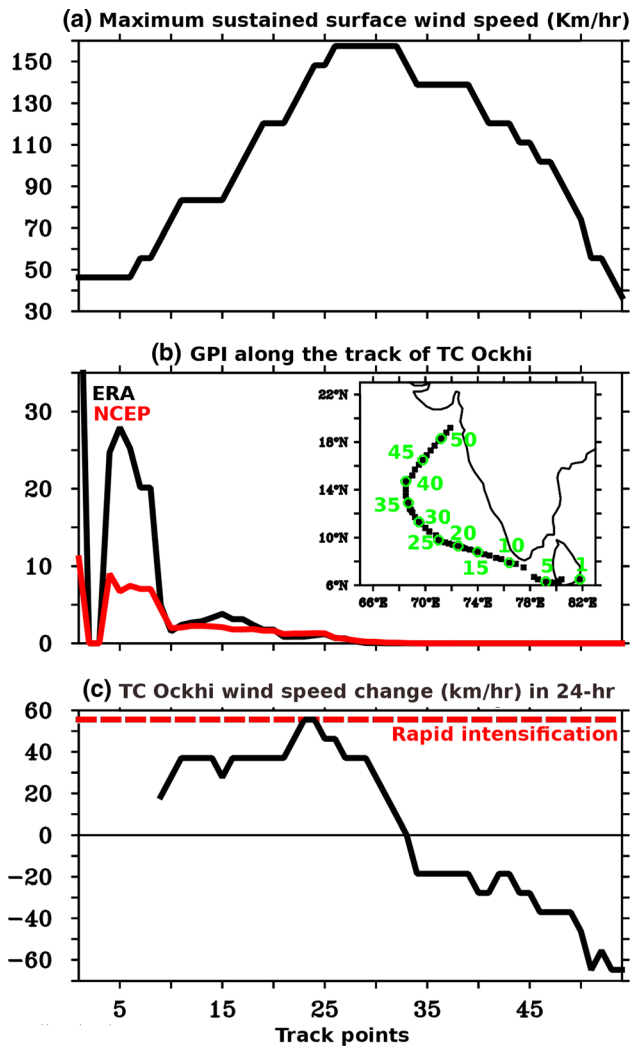


Figure 12. (a) Maximum sustained wind speed along the track of TC-Ockhi, (b) GPI intensity with respect to TC-Ockhi location and (c) 24-hr wind speed change of TC-Ockhi along the track. Track points are the points 1–50 marked along the track of TC-Ockhi shown in (b).

boxes as shown in figure 1 to understand the GPI characteristics and to unravel the special features during this period. The track of TC-Ockhi is also overlaid along with its different stages and the corresponding dates labelled in the same figure for easy reference and correlation. India Meteorological Department clearly forecasted the cyclogenesis. However, the rapid intensification of TC in the above-mentioned region, particularly box 2, was not able to be forecasted well (IMD 2017). When the TC presence was clarified in box 2, TC-Ockhi forecast was reasonably good further.

Our analysis further shows that in the top of background conditions, primarily low-level vorticity and secondarily mid-tropospheric relative humidity were the dominant contributing factors, which lead to an enhanced GPI during the

TC-Ockhi period (figure 10). Figure 11 represents temporal evolution of GPI anomaly (derived using ERA Interim data) during pre-TC-Ockhi period (during 20–28 November) in different boxes as indicated in figure 1. Figure 11 depicts that the GPI has an increasing trend with respect to the climatology from 22 November, particularly in boxes 1 and 2. That is, four days before the genesis of TC-Ockhi, the environmental factors were above normal in boxes 1 and 2 (figure 11), and hence conducive for the formation of this TC. It may be reiterated that our analysis is consistent in both NCEP and ERA-interim reanalysis products.

Another important question was whether the TC-Ockhi intensification rate was unusual in comparison with the general trend of the TC formation and intensification rate in the AS. Also, a question to be addressed was that whether such an unusual behaviour might have led to an inaccurate forecast on the intensification rate of TC-Ockhi during the first three days of the system. Figure 12 represents the maximum sustained wind speed along the track of TC, GPI intensity with respect to TC-Ockhi location and 24-hr wind speed change of TC-Ockhi. The figure shows that the TC-Ockhi had an intensification tendency until it crossed the high GPI region (compare figure 10, figure 11-GPI climatology and GPI anomaly before TC-Ockhi and figure 1 depicting track with TC category transformation timings and selected boxes) and it had a decaying tendency while it entered and traversed through the region of low GPI.

Figure 13 shows the frequency histogram of time taken for TCs to develop from Depression (D) to Cyclonic Storm (CS) and Deep Depression (DD) to CS. Data on the cyclones from 1980 were taken from the IMD E-Atlas for this analysis. As evident from figure 14, the majority (22 out of 29; 73%) of TC intensified from D to CS within 24 hrs. It is to be noted that the peak 6-hr period of TC intensified from D to CS is 18–24 hr (9 out of 29; 30%). If we look into the time taken from DD to CS, majority of TC took 3–6 hrs to develop from DD to CS (8 out of 29; 27%). Similarly, very few cyclones (3 out of 29 cyclones) intensified taking durations between 0 and 3 hrs. This indicates that around 37% (11 out of 29 TC) TC intensified from DD to CS within 6 hrs. TC-Ockhi has taken 24 hrs to intensify from D to CS and 6 hrs from DD to CS (TC-Ockhi is marked as red dot in figure 13), which falls under the time period where majority of TC cases fall. This analysis indicates that the TC-Ockhi also had rapid intensification in a similar fashion the earlier cyclones in this region behaved.

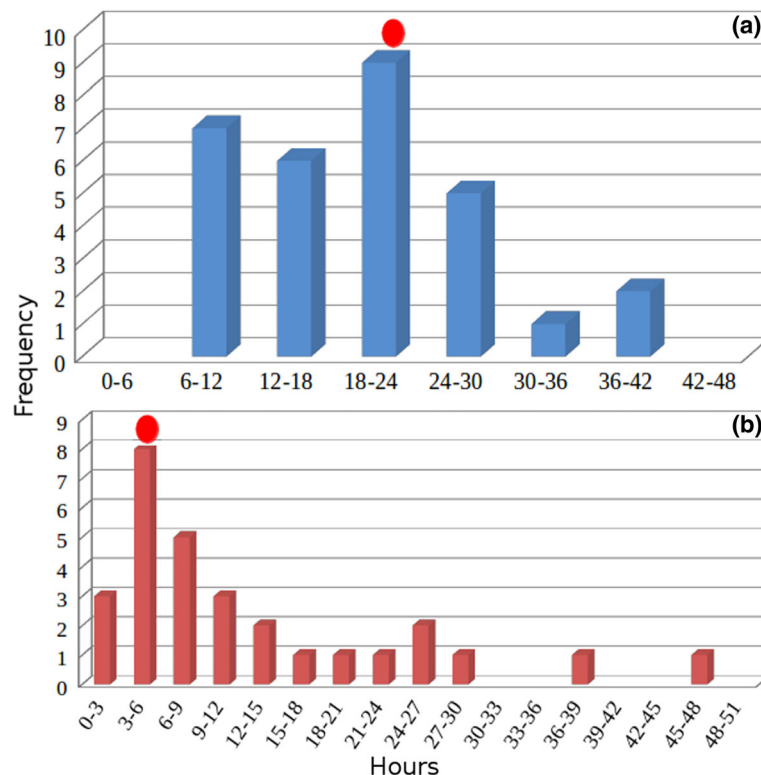


Figure 13. (a) Frequency histogram of time taken for TC to develop from D to CS and (b) DD to CS. Red circle indicates TC-Ockhi.

Track of the TC generally follows the background tropical flow and Beta drift. Earlier studies have shown that in the absence of environmental steering, the Northern Hemisphere TCs move towards the northwest with a speed of about several degrees per day due to the equatorial beta effect (Chan and Williams 1987; Williams and Chan 1994). The upper airflow pattern that prevails in the cyclone period is the most dominant external factor (80–90%) influencing the TC movement (Chan and Gray 1982; Neumann 1992). Following Velden and Leslie (1991), Tropospheric wind (850–200 hPa) averaged over the time period of 30 days with centre at 29 November 2017 shows a north-eastward trend beyond 14 deg north (figure 14). Average of the same parameter for a period of 24–28 November 2017 also shows an eastward trend beyond 16 deg north. So, TC-Ockhi has made a turn towards Indian coastline towards Maharashtra coast. The track of TC-Ockhi matches well with the background tropospheric flow (wind averaged over 850–200 hPa), so, in broad sense, there are no abnormalities in the track of TC-Ockhi.

In short, the climatological analyses suggest that the southeastern AS region, where the TC-Ockhi was intensified, is seen to have all the favourable

conditions to get the system intensified during November–December months. With respect to the annual mean, during November and December months, vorticity and wind shear play a dominant role on the TC genesis in the Arabian Sea and southwest Bay of Bengal. Early studies have shown that ENSO and MJO can significantly modulate TC activity in the northern Indian Ocean, such that both La Nina and active phase of MJO provide favourable conditions for TC genesis and intensification (Girishkumar and Ravichandran 2012; Girishkumar *et al.* 2015). Singh *et al.* (2020) showed that the MJO and warm oceanic conditions provided favourable dynamic and thermodynamic conditions for the genesis of cyclone Ockhi. There are past studies (Saha 2009; Geetha and Balachandran 2014; Sanap *et al.* 2018), which depict the role of easterly waves and their association with ENSO, in forming the synoptic systems over northern Indian Ocean, especially over the Bay of Bengal. However, Sanap *et al.* (2020) suggest that the Easterly Wave (MJO) played a seminal (insignificant) role in preconditioning the atmosphere for the cyclogenesis of the Ockhi. In fact, the period of TC-Ockhi coincides with the La Nina event in the Pacific and westward propagation of the active phase of the MJO in the Indian



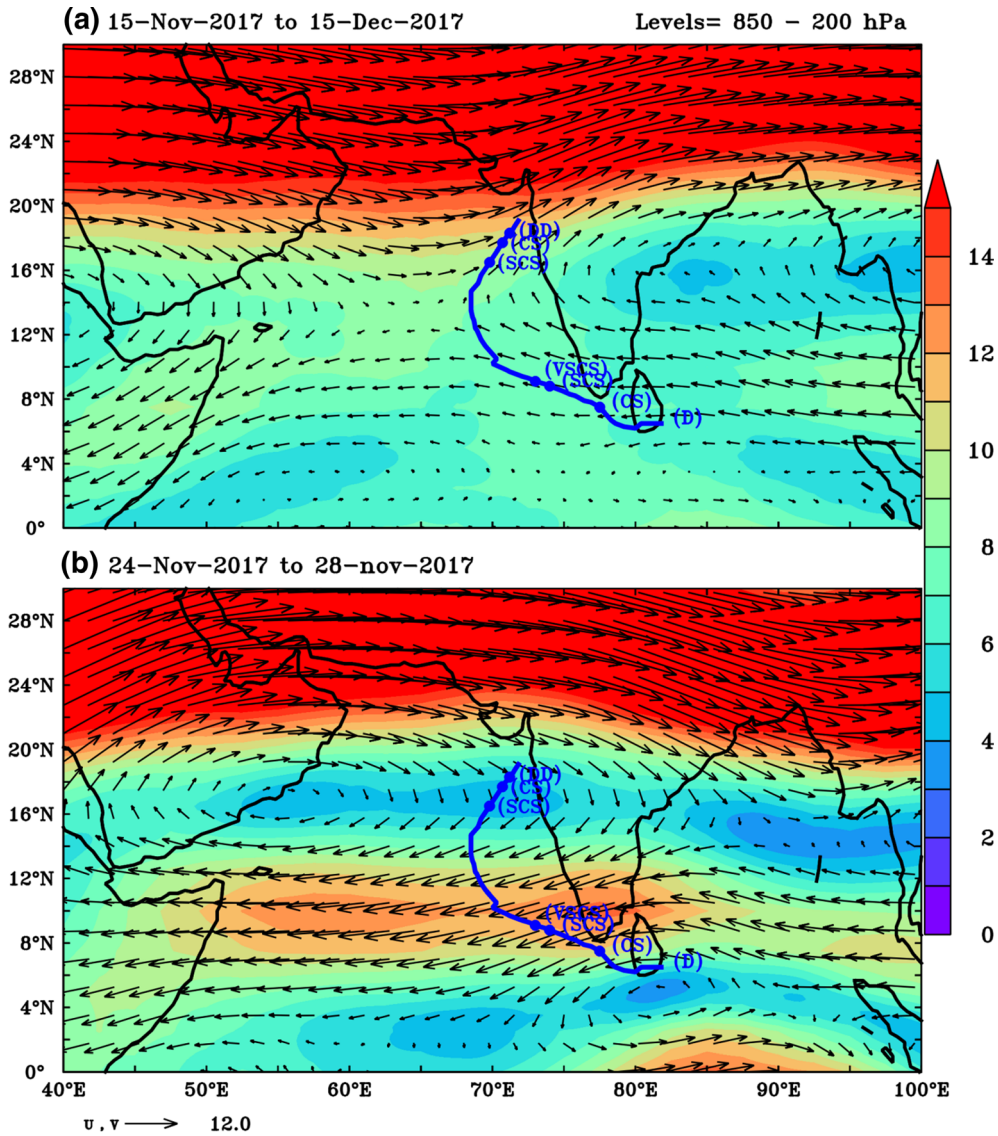


Figure 14. Tropospheric wind [m/s, 850–200 hPa averaged] (a) averaged over the time period of 30 days with centre at 29 November 2017 and (b) averaged for a period of 24–28 November 2017.

Ocean. The presence of these two modes may be the plausible reason for the enhancement of background condition in the Arabian Sea and southwest Bay of Bengal before the formation of TC-Ockhi. However, more detailed analyses are required to quantify the role of these synoptic activities on this kind of enhancement observed, which would have eventually led to the intensification of the TC-Ockhi.

#### 4. Conclusion

Ocean state forecasting in terms of forecasts of significant wave height, swell wave height, wind sea wave height, maximum wave height, mean wave period, mean wave direction generated at

INCOIS from a numerical spectral wave model and also wind speed and wind direction are evaluated using the available open ocean moored buoys and coastal DWRBs in the present study. Characteristics of TC-Ockhi in terms of its genesis, intensity and track compared to other cyclones in the past were also unravelled in a forecasting perspective.

In the Arabian Sea, the forecasts of wave parameters from the model forced with bias-corrected ECMWF winds resulted in very good agreement with observations. Bias is <0.2 m in case of wave heights, and the scatter index for all the wave parameters were in the range of 15–30% with *r* values varying from 0.78 to 0.95 and the RMSE ranges 0.33–0.36 m in case of *H<sub>s</sub>*, *H<sub>sw</sub>* and *H<sub>ss</sub>*, indicating a very good agreement of forecasts with observation in the open ocean. The accuracy

of coastal forecasts was separately assessed as its impact on the coastal population is pertinent. Forecasted coastal waves have bias in the range  $\sim 0.02$  m for Hs, 0.14 s for Tp,  $0.33^\circ$  for Pdir, and RMSE values are in the range 0.2 m for Hs, 1.5 s for Tp and  $24^\circ$  for Pdir. The scatter index varied from 16 to 22% with high correlation with  $r$  of 0.76–0.95 suggesting a good agreement of the coastal wave forecasts also during this cyclone period. Bias-corrected winds show good agreement with the observation with a bias of only 0.08 m/s and RMSE of 0.33 m/s in the AS. It was also found out that the Hs and the wave power near the Agatti Islands were contributed from both wind seas and swell seas before and after the arrival of the cyclone, while it is mainly from the wind sea only during the period 1st–2nd December due to the influence of cyclone in this region.

In general, during the November and December months, GPI is very high in the southeastern Arabian Sea, south of Indian peninsula and east of Sri Lanka. Present study revealed that, climatologically, these regions have large potential for the genesis and intensification of TC, mainly due to an enhanced low-level cyclonic vorticity and the reduction in vertical wind shear. During the TC-Ockhi period, on top of background conditions, low-level vorticity and mid-tropospheric relative humidity were the dominant contributing factors, which lead to an enhanced GPI in the Arabian Sea. Another finding is that the TC-Ockhi also had rapid intensification in a similar fashion the earlier cyclones in this region behaved. The TC-Ockhi track matches with the background tropospheric flow (wind averaged over 850–200 hPa) as expected in general.

In the context of predicting the track and intensity of the TC-Ockhi by models, there was no forecasted (issued on 27 November) clue on the intensification of the depression on 29 November (IMD 2017). But, it was forecasted (issued on 28 and 29 November, based on the updated initial conditions) to get intensified the system during successive days. Hence, it is worth mentioning here that, the above understanding about the system in terms of GPI and other characteristics could have helped the cyclone forecasters to presume that the system would get intensified than getting weakened, during the successive days, though the models could not predict it well. So, the present study suggests that the forecasters should look into and analyse extensively the background dynamic and thermodynamic conditions in addition to

multi-model guidance to better predict the genesis, intensity and track of the cyclones without any miss or false alarm. In the present scenario of global warming on the wake of climate change, there are increased reports in the recent past on the consequential increase in the intensity and frequency of extreme weather and oceanic hazards. In this context, studies similar to the present one would throw more light into our understanding about the evolving earth system, which would, in turn, help us to combat the natural hazards appropriately and sustainably without leading it to a disaster.

### Acknowledgements

Authors are thankful to the Director, INCOIS and the Secretary, MoES, Govt of India for support. Thanks are also due to the FERRET (NCEP) team, which was used in this paper for data analysis and visualisation. NCEP and ECMWF (ERA-interim data) are thanked for providing the data. We thank two anonymous reviewers for their constructive comments and suggestion on the manuscript and its eventual improvement. Special thanks to the editor for his valuable comments and editorial corrections. This is INCOIS contribution no. 448.

### Author statement

RH conceived the idea, planned, analysed, organised and wrote the manuscript. PS and SV supported in writing the manuscript. AM, MSG, TMB and MM supported in the data analysis and interpretations. RK, YG and DKP helped to plot the figures.

### Appendix

Motivated from the work of Gray (1979), Emanuel and Nolan (2004) developed an empirical index named the Genesis Potential Index (GPI) to quantitatively describe the influence of large-scale environmental features on the TC genesis. Following, Emanuel and Nolan (2004), GPI can be represented as follows:

$$\text{GPI} = \left(\frac{H}{50}\right)^3 \times |10^5 \eta|^{\frac{3}{2}} \times (1 + 0.1 V_{\text{shear}})^{-2} \times \left(\frac{V_{\text{pot}}}{70}\right)^3, \quad (1)$$

where  $H$  is the relative humidity (%) at 600 hPa,  $\eta$  is the absolute vorticity at 850 hPa ( $\text{s}^{-1}$ ),  $V_{\text{shear}}$  is the magnitude of the vertical wind shear ( $\text{m s}^{-1}$ ) between 850 and 200 hPa, and  $V_{\text{pot}}$  is the maximum TC potential intensity (PI) ( $\text{m s}^{-1}$ ) defined by Emanuel (1999 and reference therein). The normalizing factors make the GPI dimensionless and the values were selected to keep the individual terms within the same order of magnitude.

For ease computation of relative roles of large-scale environmental factors to the total changes in the GPI, Li *et al.* (2013) modified the GPI equation as:

$$\delta\text{GPI} = \alpha_1 \times \delta\left(\frac{H}{50}\right)^3 + \alpha_2 \times \delta|10^5\eta|^{\frac{3}{2}} + \alpha_3 \times \delta(1 + 0.1V_{\text{shear}})^{-2} + \alpha_4 \times \delta\left(\frac{V_{\text{pot}}}{70}\right)^3, \quad (2)$$

where

$$\alpha_1 = \overline{|10^5\eta|^{\frac{3}{2}}} \times \overline{(1 + 0.1V_{\text{shear}})^{-2}} \times \overline{\left(\frac{V_{\text{pot}}}{70}\right)^3},$$

$$\alpha_2 = \overline{\left(\frac{H}{50}\right)^3} \times \overline{(1 + 0.1V_{\text{shear}})^{-2}} \times \overline{\left(\frac{V_{\text{pot}}}{70}\right)^3},$$

$$\alpha_3 = \overline{\left(\frac{H}{50}\right)^3} \times \overline{|10^5\eta|^{\frac{3}{2}}} \times \overline{\left(\frac{V_{\text{pot}}}{70}\right)^3}$$

and

$$\alpha_4 = \overline{\left(\frac{H}{50}\right)^3} \times \overline{|10^5\eta|^{\frac{3}{2}}} \times \overline{(1 + 0.1V_{\text{shear}})^{-2}}.$$

In the above expressions, the horizontal bar indicates mean state (climatology) and  $\delta$  represents the perturbation (anomaly) of the individual parameter.

## References

Akhila G N and Anna Durai R 2018 A study on various tropical cyclone hits in India through GIS approach; *Int. J. Pure Appl. Math.* **119** 589–595.

Balakrishnan Nair T M, Remya P G, Harikumar R, Sandhya K G, Sirisha P, Srinivas K, Nagaraju C, Arun N, Krishna Prasad B, Jeyakumar C, Kaviyazhahu K, Hithin N K, Rakhi Kumari, Sanil Kumar V, Ramesh Kumar M, Sheno S S C and Shailesh Nayak 2014 Wave forecasting and monitoring during very severe cyclone Phailin in the Bay of Bengal; *Curr. Sci.* **106**(8) 1121–1125.

Balakrishnan Nair T M, Sirisha P, Sandhya K G, Srinivas K, Sanil Kumar V, Sabique L, Arun N, Krishna Prasad B, Rakhi Kumari, Jeyakumar C, Kaviyazhahu K, Ramesh Kumar M, Harikumar R, Sheno S S C and Shailesh Nayak 2013 Performance of the Ocean State Forecast system at Indian National Centre for Ocean Information Services; *Curr. Sci.* **105**(2) 175–181.

Camargo S J, Emanuel K A and Sobel A H 2007 Use of a genesis potential index to diagnose ENSO effects on tropical cyclone genesis; *J. Clim.* **20** 4819–4834.

Chan J C L and Gray W M 1982 Tropical cyclone movement and surrounding flow relationships; *Mon. Weather Rev.* **110** 1354–1374, [https://doi.org/10.1175/1520-0493\(1982\)110<1354:TCMASF>2.0.CO;2](https://doi.org/10.1175/1520-0493(1982)110<1354:TCMASF>2.0.CO;2).

Chan J C L and Williams R T 1987 Numerical studies of the beta effect in tropical cyclone motion. Part I: Zero mean flow; *J. Atmos. Sci.* **44** 1257–1265, [https://doi.org/10.1175/1520-0469\(1987\)044<1257:AANSOT>2.0.CO;2](https://doi.org/10.1175/1520-0469(1987)044<1257:AANSOT>2.0.CO;2).

Dee D P, Uppala S M and Simmons A J 2011 The ERA-Interim reanalysis: Configuration and performance of the data assimilation system; *Quart. J. Roy. Meteor. Soc.* **137**(656) 553–597.

Emanuel K A 1999 Thermodynamic control of hurricane intensity; *Nature* **401** 665–669, <https://doi.org/10.1038/44326>.

Emanuel K A and Nolan D S 2004 Tropical cyclone activity and the global climate system; In: 26th Conf. on Hurricanes and Tropical Meteorology, *Miami FL Am. Meteor. Soc. A* **10** 240–241.

Evan A T and Camargo S J 2011 A climatology of Arabian Sea cyclonic storms; *J. Climate* **24**, <https://doi.org/10.1175/2010JCLI3611.1>.

Geetha B and Balachandran S 2014 An analytical study of easterly waves over southern peninsular India during the northeast monsoon 2010; *Mausam* **65**(4) 591–602.

Girishkumar M S and Ravichandran M 2012 The influences of ENSO on tropical cyclone activity in the Bay of Bengal during October–December; *J. Geophys. Res.* **117**(C02033) 1–13, <https://doi.org/10.1029/2011JC007417>.

Girishkumar M S, Suprit K, Vishnu S, Thanga Prakash V P and Ravichandran M 2015 The role of ENSO and MJO on rapid intensification of tropical cyclones in the Bay of Bengal during October–December; *Theor. Appl. Climatol.* **120** 797–810, <https://doi.org/10.1007/s00704-014-1214-z>.

Gray W M 1979 Hurricanes: Their formation, structure and likely role in the tropical circulation. Meteorology over the tropical oceans; *Roy. Meteor. Soc.* **77** 155–218.

Harikumar R, Balakrishnan Nair T M, Rao B M, Rajendra Prasad P, Ramakrishna Phani P, Nagaraju C, Ramesh Kumar M, Jeyakumar C, Sheno S S C and Shailesh Nayak 2016 Ground zero met-ocean observations and attenuation of wind energy during Cyclonic Storm Hudhud; *Curr. Sci.* **110**(12) 2245–2252, <https://doi.org/10.18520/cs/v110/i12/2245-2252>.

Harikumar R, Hithin N K, Balakrishnan Nair T M, Sirisha P, Krishna Parasad B, Jeyakumar C, Shailesh Nayak and Sheno S S C 2015 Ocean State Forecast along ship-routes: Evaluation using ESSO-INCOIS real-time ship-mounted wave height meter and satellite observations; *J. Atmos. Oceanic Technol.* **32**(11) 2211–2222, <https://doi.org/10.1175/JTECH-D-15-0047.1>.

- Hithin N K, Remya P G, Balakrishnan Nair T M, Harikumar R, Raj Kumar and Shailesh Nayak 2015 Validation and inter-comparison of SARAL/AltiKa and PISTACH derived coastal wave heights using *in-situ* measurements; *IEEE Trans. Geosci. Rem. Sens.* **99** 1–10, <https://doi.org/10.1109/JSTARS.2015.2418251>.
- IMD 2017 Very Severe Cyclonic Storm “Ockhi” over Bay of Bengal (29 November–06 December 2017): A Report; <http://www.rsmcnewdelhi.imd.gov.in/images/pdf/publications/preliminary-report/cs29nov-06dec.pdf>.
- Kalnay E, Kanamitsu M and Kistler R 1996 The NCEP/NCAR 40-year reanalysis project; *Bull. Am. Meteor. Soc.* **77** 437–470.
- Li Z W, Yu W, Li T, Murty V S N and Tangang F 2013 Bimodal character of cyclone climatology in the Bay of Bengal modulated by monsoon seasonal cycle; *J. Clim.* **26** 1033–1046.
- Neumann C J 1992 The Joint Typhoon Warning Center (JTWC92) model, Final Rep. N00014-90-C-6042; Sci. Appl. Int. Corp., Monterey Calif, 85.
- Saha K 2009 *Tropical circulation systems and monsoons*; Springer Science & Business Media, 329p.
- Sanap S D, Mohapatra M, Ali M M, Priya P and Varaprasad D 2020 On the dynamics of cyclogenesis, rapid intensification and recurvature of the very severe cyclonic storm, Ockhi; *J. Earth Syst. Sci.* **129** 194, <https://doi.org/10.1007/s12040-020-01457-2>.
- Sanap S D, Priya P, Sawaisarje G and Hosalikar K S 2018 Heavy rainfall events over south-east peninsular India during north-east monsoon: Role of El-Niño and easterly wave activity; *Int. J. Climatol.* **39**(4) 1954–1968, <https://doi.org/10.1002/joc.5926>.
- Singh V K, Roxy M K and Deshpande M 2020 The unusual long track and rapid intensification of very severe cyclone Ockhi; *Curr. Sci.* **119**(5) 771–779. <https://doi.org/10.18520/cs/v119/i5/771-779>.
- Sirisha P, Remya P G, Balakrishnan Nair T M and Rao B V 2015 Numerical simulation and observations of very severe cyclone generated surface wave fields in the north Indian Ocean; *J. Earth Syst. Sci.* **124**(8) 1639–1651.
- Sirisha P, Sandhya K G, Balakrishnan Nair T M and Rao B 2017 Evaluation of wave forecast in the north Indian Ocean during extreme conditions and winter monsoon evaluation of wave forecast in the north Indian Ocean during extreme conditions and winter monsoon; *J. Oper. Ocean.* **10**(1) 79–92, <https://doi.org/10.1080/1755876X.2016.1276424>.
- Thara K G 2018 India/Cyclone Ockhi: A stitch in time; *Samudra Report* **78** 10–14.
- Velden C S and Leslie L M 1991 The basic relationship between tropical cyclone intensity and the depth of the environmental steering layer in the Australian region; *Wea. Forecasting* **6**, [https://doi.org/10.1175/1520-0434\(1991\)006<0244:TBRBTC>2.0.CO;2](https://doi.org/10.1175/1520-0434(1991)006<0244:TBRBTC>2.0.CO;2).
- Williams R T and Chan J C L 1994 Numerical studies of the beta effect in tropical cyclone motion. Part II: Zonal mean flow effects; *J. Atmos. Sci.* **51** 1065–1076, [https://doi.org/10.1175/1520-0469\(1994\)051<1065:NSOTBE>2.0.CO;2](https://doi.org/10.1175/1520-0469(1994)051<1065:NSOTBE>2.0.CO;2).
- Zhang T, Lin W, Lin Y, Zhang M, Yu H, Cao K and Xue W 2019 Prediction of tropical cyclone genesis from mesoscale convective systems using machine learning; *Wea. Forecasting* **34** 1035–1049, <https://doi.org/10.1175/WAF-D-18-0201.1>. [https://incois.gov.in/WEBSITE\\_FILES/OSF\\_FILES/forecast/Bulletins](https://incois.gov.in/WEBSITE_FILES/OSF_FILES/forecast/Bulletins). <http://www.rmchennaieatlas.tn.nic.in>

Corresponding editor: C GNANASEELAN